The Plant Cell, Vol. 9, 2271–2280, December 1997

Biochemical Characterization of Arabidopsis Wild-Type and Mutant Phytochrome B Holoproteins

Tedd D. Elich [1] and Joanne Chory [2]

Howard Hughes Medical Institute, Plant Biology Laboratory, Salk Institute for Biological Studies, 10010 North Torrey Pines Road, La Jolla, California 92037

Although phytochrome B (phyB) plays a particularly important role throughout the life cycle of a plant, it has not been studied in detail at the molecular level due to its low abundance. Here, we report on the expression, assembly with chromophore, and purification of epitope-tagged Arabidopsis phyB. In addition, we have reconstructed two missense mutations, phyB-4 and phyB-101, isolated in long hypocotyl screens. We show that mutant proteins phyB-4 and phyB-101 exhibit altered spectrophotometric and biochemical properties relative to the wild-type protein. In particular, we demonstrate that phyB-101 Pfr exhibits rapid nonphotochemical (dark) reversion to Pr that results in a lower photoequilibrium level of the active Pfr form. We conclude that this occurs in vivo as well because *phyB-101* mutants are shown to lack an end-of-day–far-red hypocotyl elongation response that requires a stable Pfr species. We propose that this Pfr instability may be the primary molecular mechanism underlying the *phyB-101* mutant phenotype.

INTRODUCTION

The ambient light environment influences the growth and development of plants throughout their life cycle. There are three major classes of regulatory photoreceptors involved in mediating responses to light in plants: UV-B receptors, blue/UV-A receptors, and a family of red/far-red (FR) receptors known as phytochromes (Quail et al., 1995; Fankhauser and Chory, 1997). Of these, phytochromes were the first photoreceptors purified, and phytochromes remain the most widely studied and best characterized regulatory receptors in plants.

Phytochromes are large, soluble proteins that exist as dimers in solution. Each monomer is ~120 kD and contains a single, covalently attached linear tetrapyrrole chromophore responsible for the absorption of visible light. Phytochromes have the unique ability to exist in two spectrally and biochemically distinct forms: a red light–absorbing form called Pr and a FR light–absorbing form called Pfr. These two forms are photointerconvertible, so that red light converts Pr to Pfr and FR light converts Pfr to Pr (Elich and Chory, 1994; Quail et al., 1995). This phototransformation involves a Z,syn-to-E,anti-isomerization of the C_{15} carbon between the C and D chromophore pyrrole rings, and this isomerization is coupled to a rearrangement of the protein backbone (Andel et al., 1996). The Pfr form is generally accepted to be the active form of the molecule, because classic low-fluence phytochrome responses are red light inducible and FR light reversible.

The phytochrome molecule folds into two major domains separated by a protease-sensitive hinge region: an ~70-kD N-terminal chromophore-bearing domain and an ~55-kD C-terminal domain. The C-terminal domain contains a proximal PAS homology domain that is delimited by two direct repeats showing sequence similarity to the repeats that define PAS domains (Lagarias et al., 1995; Kay, 1997). (PAS is an acronym derived from the initial three proteins observed to contain this polypeptide motif: the *period* gene product of fruit flies, the aryl hydrocarbon receptor nuclear transporter, and the *single-minded* gene product of fruit flies.) The phytochrome C terminus also contains a distal histidine kinase homology domain that shows sequence similarity with transmitter modules of bacterial two-component systems (Schneider-Poetsch, 1992). Regions of the histidine kinase homology domain are necessary for dimerization and biological activity (Cherry et al., 1993), whereas the PAS homology domain is a hotspot for missense mutations that affect phytochrome function (Quail et al., 1995).

Phytochromes are encoded by small multigene families in all organisms examined in detail. In Arabidopsis, this family comprises five genes, *PHYA* to *PHYE* (Quail et al., 1995). The isolation of phytochrome mutants in this plant has allowed the assignment of specific functions to different phytochromes. For example, phyA is known to mediate nonreversible, very-low-fluence responses for seed germination and *cab* (gene for the light-harvesting chlorophyll *a/b* binding protein) induction (Shinomura et al., 1996; Hamazato et al., 1997) as well as a FR high-irradiance response for the inhibition of hypocotyl elongation (Nagatani et al., 1993; Parks

[1] Current address: Monsanto Company, 700 Chesterfield Village Parkway, Chesterfield, MO 63198.
[2] To whom correspondence should be addressed. E-mail chory@salk.edu; fax 619-558-6379.

and Quail, 1993; Whitelam et al., 1993). In comparison, phyB is known to mediate reversible low-fluence responses for *cab* induction and seed germination (Shinomura et al., 1996; Hamazato et al., 1997) and end-of-day–FR (EOD-FR) effects on hypocotyl elongation (Robson et al., 1993). Currently, it is not known whether such functional specificity is due to differences in intrinsic biochemical and photochemical properties or to nonintrinsic properties, such as differences in absolute protein levels or spatial and temporal expression patterns. One obvious reason for this lack of knowledge is that only phyAs have been purified and extensively characterized due to their relative abundance in etiolated tissue.

Recombinant protein expression systems offer an alternative source of the less abundant phytochromes. In particular, yeast expression systems have proven to be the most useful for the expression of the native phytochrome apoprotein that is competent for chromophore attachment (Wahleithner et al., 1991). Recently, the fusion of a nine–amino acid "Strep-tag" (a peptide with intrinsic streptavidin binding activity) to full-length oat phyA was employed to purify to apparent homogeneity recombinant phytochrome for the first time (Murphy and Lagarias, 1997). The purified recombinant fusion protein had biochemical and spectrophotometric properties indistinguishable from the native photoreceptor purified from plants (Murphy and Lagarias, 1997). Here, we employed this system to purify recombinant Arabidopsis phyB for biochemical and spectrophotometric characterization. In addition, to gain insight into structure–function relationships, we reconstructed in our expression system for comparative analysis two *phyB* missense mutations, phyB-4 and phyB-101, isolated from long hypocotyl mutant screens. In this article, we demonstrate that both of the mutant proteins exhibited altered spectrophotometric and biochemical properties, and we discuss the implications of these results with respect to phytochrome function.

RESULTS

phyB Mutants

There are two *phyB* missense mutations isolated in long hypocotyl screens, both in the Landsberg *erecta* (L*er*) background, for which plants are available: *phyB-4* (Reed et al., 1993) and *phyB-101* (Bradley et al., 1996). The *phyB-4* mutation results in a His-to-Tyr change at amino acid 283, which lies in the photosensory domain in proximity to the chromophore binding site at position 352. The *phyB-101* mutation causes a Glu-to-Lys change at amino acid 812, which lies in the second of the two direct repeats that define the PAS homology domain (Lagarias et al., 1995; Kay, 1997). The identical mutation was also recovered in a screen for intragenic suppressors of an overexpressing *PHYB* transgene (Wagner and Quail, 1995). Interestingly, the PAS homology domain is a mutation hotspot, containing 16 of 22 known *phyA* and *phyB* missense mutations (Quail et al., 1995).

Six-day-old continuous white light–grown seedlings of wild-type L*er*, *phyB-4*, *phyB-101*, and *phyB-1* (a null allele in the L*er* background; Reed et al., 1993) are shown in Figure 1. Seedlings with missense alleles display intermediate phenotypes relative to L*er* and *phyB-1* control seedlings, demonstrating that both *phyB-4* and *phyB-101* retain some phyB activity. Under most conditions, hypocotyl measurements show that the *phyB-101* phenotype is slightly more severe than that of *phyB-4*, with the magnitude of the difference depending on the exact conditions used (data not shown). To determine whether reductions in phyB activity could be due to changes in phyB protein levels, immunoblot analysis of total protein extracts from L*er* and *phyB* seedlings was performed. Both *phyB-4* and *phyB-101* plants were found to contain normal PhyB protein levels (Figure 2). The specificity of the antibodies was demonstrated by the lack of a band in the *phyB-1* negative control (Figure 2).

Phytochrome Expression, Assembly with Chromophores, and Purification

Next, we decided to determine whether phyB-4 and phyB-101 were impaired in chromophore attachment or photoreversibility. Due to the low levels of phyB in plants, we turned to a yeast expression system as a source of protein for these studies. The two *phyB* missense mutations were re-

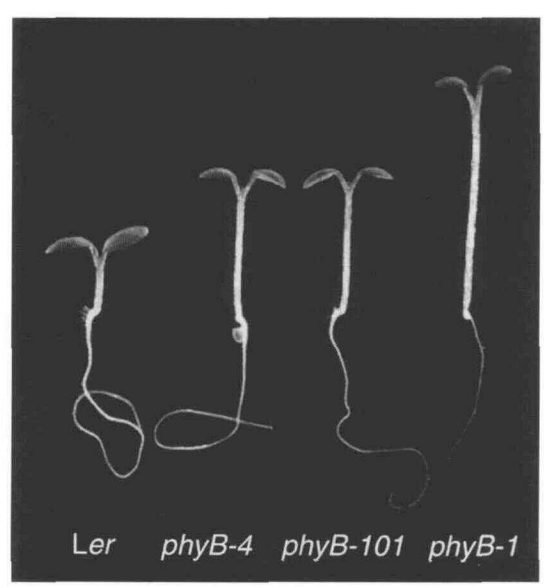

Figure 1. Six-Day-Old Wild-Type and *phyB* Seedlings.

Shown are a wild-type (L*er*) seedling (left) and three *phyB* seedlings grown under continuous white light.

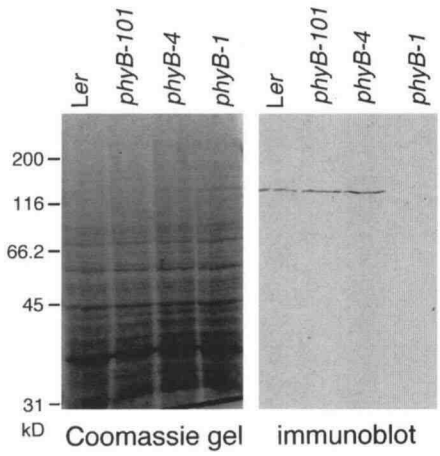

Figure 2. Immunoblot Analysis of Wild-Type and *phyB* Plants.

Whole-plant extracts of 6-day-old etiolated wild-type and *phyB* seedlings were analyzed by SDS-PAGE followed by Coomassie blue staining (left) or immunoblotting with the anti-phyB monoclonal antibody mBA2 (right). Each lane represents protein from 12 seedlings. Numbers at left indicate molecular masses in kilodaltons.

constructed in a Strep-tagged *PHYB* cDNA, and the wild-type and mutant genes were cloned into an inducible yeast expression vector. Previous studies with oat phyA have shown that this peptide tag does not significantly affect phytochrome's biochemical or spectrophotometric properties (Murphy and Lagarias, 1997). In addition, we have found that this tag does not significantly affect phytochrome function, because a transgene encoding a PhyB–Strep-tag fusion was able to rescue the seedling defects in a *phyB* null mutant (T.D. Elich and J. Chory, unpublished data).

Galactose induction of yeast transformed with the wild-type and mutant constructs led to the expression of a predominantly full-length 129-kD protein (Figure 3) that comigrated with plant-extracted phyB in all cases (data not shown). All three affinity-peptide-tagged phytochromes were capable of attaching the chromophore precursor analog phycocyanobilin (PCB) to form a photoreversible holophytochrome (see below). Yields of phyB and phyB-101 in the ammonium sulfate–precipitated fraction were generally 60 to 120 μg/L of culture. Interestingly, phyB-4 was reproducibly expressed at five- to eightfold lower levels, suggesting that this protein is less stable in yeast (although apparently not in plants; Figure 2).

The Strep-tagged holoproteins could be readily purified by binding to streptavidin–Sepharose followed by diaminobiotin elution (Figure 3). Although we have no absolute phyB standard for comparison, we could assess the relative chromophore-to-protein stoichiometry of the three PCB adducts by SDS-PAGE analysis of purified proteins that were loaded based on their A_{650}^{Pr} absorbance. Results from such experiments indicated that all three phytochromes exhibited similar chromophore-to-protein stoichiometries (Figure 3 and dilution series for which data are not shown).

Steric exclusion chromatography was performed with the Pr forms of phyB and phyB-101, and the results are presented in Table 1. The estimated molecular masses are similar to each other and consistent with a dimeric quaternary structure for phyB, as has been reported for phyAs (Lagarias and Mercurio, 1985; Jones and Quail, 1986).

Spectrophotometric Properties

Absolute absorbance and absorbance difference spectra of the Pr and Pfr forms of the three purified phytochromes are shown in Figure 4. The Pr spectra as well as the $\lambda\Delta A_{max}$ and $\lambda\Delta A_{min}$ of the three phytochromes were virtually identical, suggesting similar chromophore conformations in all cases. Nonetheless, notable differences between the mutant and wild-type proteins are apparent (Figure 4 and Table 1). In particular, although the phyB absorbance difference ratio ($\Delta A_{max}/\Delta A_{min}$) of 1.12 is very similar to the 1.14 reported for Strep-tagged recombinant oat phyA (Murphy and Lagarias, 1997), both missense mutations display considerably higher ratios. These results suggest changes in the chromophore environment, leading to alterations in the relative molar extinction coefficients of the Pr and Pfr forms. Because the Pr

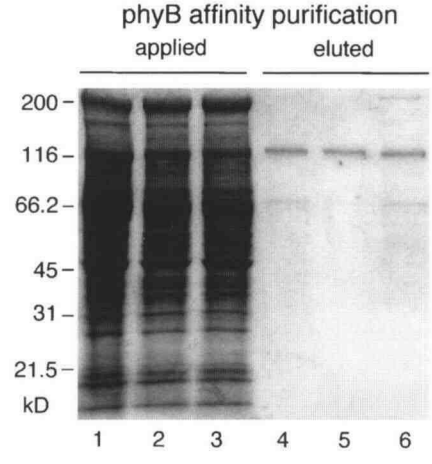

Figure 3. SDS-PAGE Analysis of the Affinity Purification of phyB, phyB-101, and phyB-4.

Shown is a Coomassie blue–stained gel showing the applied ammonium sulfate–precipitated fractions (lanes 1 to 3) and diaminobiotin-eluted and diamonobiotin-concentrated fractions (lanes 4 to 6) from streptavidin–Sepharose affinity chromatography of extracts from yeast expressing Strep-tagged phyB (lanes 1 and 4), phyB-101 (lanes 2 and 5), and phyB-4 (lanes 3 and 6). The eluted fractions were loaded based on spectrophotometric measurements and represent 280 ng of phyB. Numbers at left indicate molecular masses in kilodaltons.

Table 1. Properties of Purified PCB Adducts of phyB, phyB-4, and phyB-101

Holoprotein	$\lambda\Delta A_{max}$ (nm)	$\lambda\Delta A_{min}$ (nm)	$\Delta A_{max}/\Delta A_{min}$[a]	$A_{712}^{Pfr}/A_{650}^{Pfr}$[a]	Pr Native M_r (kD)[b]	Denatured M_r (kD)[c]
phyB	650	712	1.12 ± 0.024	0.82 ± 0.021	344	129
phyB-4	649	711	1.61 ± 0.04	0.37 ± 0.016	ND[d]	129
phyB-101	650	710	1.45 ± 0.035	0.41 ± 0.017	366	129

[a] Values are means from three (phyB and phyB-101) and two (phyB-4) independent phytochrome preparations ±SE or range, respectively.
[b] Determined by steric exclusion chromatography, as described in Methods.
[c] Determined from a 7.5% polyacrylamide gel calibrated with markers of 220, 100, 97.4, 66, and 46 kD.
[d] ND, not determined.

extinction coefficients appeared to be similar (see above), this is presumably the result of lower Pfr extinction coefficients. Alternatively, because little is known about the spectrophotometric properties of phyB, we cannot rule out the possibility that the absorbance properties of the subunits of Pr–Pfr heterodimers are different from those of the respective homodimers and therefore that differences in $\Delta A_{max}/\Delta A_{min}$ values are due to changes in the photoequilibrium level of Pfr (see below).

The most striking difference observed in the mutant phytochromes is seen in the Pfr spectra (Figure 4, dotted lines). Due to the overlapping absorbance properties of Pr and Pfr, saturating red light irradiation does not yield 100% Pfr but rather a photoequilibrium mixture of the two forms. Thus, the FR absorbance peak at ~712 nm in these spectra is attributable to the Pfr form of the molecule, whereas red absorbance at ~650 nm is due mainly to residual Pr. Figure 4 shows that both mutant phytochromes formed less "apparent" Pfr under saturating red light than did native phyB. This effect was seen in multiple independent phytochrome preparations and can be quantified as the spectral change ratio $A_{712}^{Pfr}/A_{650}^{Pfr}$ (Table 1). These results could be due in part to the lower Pfr molar extinction coefficients suggested by the increased absorbance difference ratios (see above). In addition, however, real decreases in the photoequilibrium levels of Pfr are indicated by the decreased Pr bleaching observed upon saturating red light irradiation of the mutant phyBs versus that seen for wild-type phyB (Figure 4; data not shown). The most plausible causes for decreases in the photoequilibrium level of Pfr include changes in the relative quantum yields for the two phototransformation reactions or changes in competing nonphotochemical reactions.

phyB Dark Reversion

The nonphotochemical reversion of Pfr to Pr (dark reversion) is easily measured and reflects Pfr thermal stability. Dark reversion measurements with ammonium sulfate–precipitated fractions of phyB, phyB-4, and phyB-101 under identical in vitro conditions are shown in Figure 5. Wild-type phyB showed moderate dark reversion similar to that reported for recombinant tobacco phyB in vivo in yeast cells (Kunkel et al., 1993). In contrast, phyB-101 exhibited extremely rapid dark reversion, with 50% of the total Pfr reverting to Pr within 6 to 7 min. Although phyB-4 also showed faster dark reversion than did phyB, the difference was much less dramatic than that seen with phyB-101, and it was only obvious after ~30 to 60 min. Very similar relative differences in dark reversion were

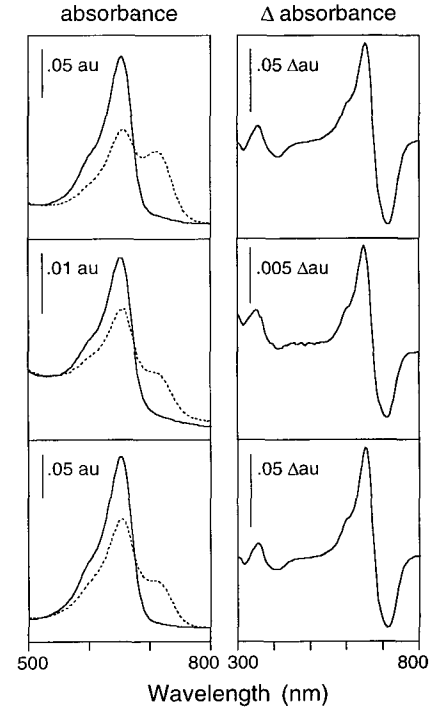

Figure 4. Absolute Absorbance and Absorbance Difference Spectra of phyB, phyB-4, and phyB-101.

Shown are Pr (solid lines) and Pfr (dashed lines) absolute absorbance spectra (left) and Pr–Pfr difference spectra (right) of PCB adducts of affinity-purified phyB (top), phyB-4 (center), and phyB-101 (bottom). au, absorbance units.

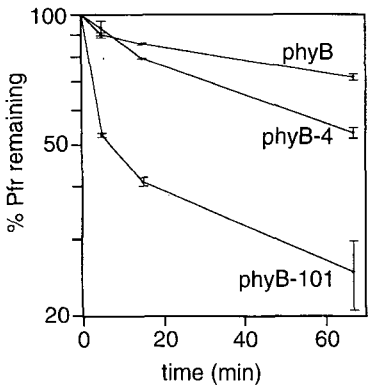

Figure 5. Dark Reversion of phyB, phyB-4, and phyB-101.

Dark reversion measurements were done with ammonium sulfate–precipitated fractions, and each value represents the mean (range indicated by error bars) of two determinations with independent phytochrome preparations.

observed when experiments were performed with purified phytochrome preparations, although the rates of reversion were somewhat faster in all cases (data not shown). Because dark reversion is known to be influenced by the exact conditions used, such differences are not unexpected, and we present the ammonium sulfate–precipitated fraction results only because we have multiple independent measurements.

In addition to decreasing the lifetime of the biologically active Pfr form, rapid dark reversion contributes to a lower photoequilibrium level of Pfr. Thus, if rapid dark reversion occurred in vivo, it would be expected to impair phytochrome activity.

phyB-101 Seedlings Lack an EOD-FR Response

Although the levels of phyB in plants are too low to measure dark reversion rates directly in vivo, phytochrome responses that show EOD-FR effects can be used for indirect measurements of this property. Studies comparing wild-type L*er* to *phyB-1* mutants have shown that the EOD-FR effect on hypocotyl elongation in Arabidopsis seedlings is mediated predominantly by phyB (Robson et al., 1993). Therefore, we performed similar experiments but included *phyB-4* and *phyB-101* in our analysis. Consistent with the previous study (Robson et al., 1993), EOD-FR treatments resulted in substantial increases in the hypocotyl length of L*er* seedlings while having no effect on *phyB-1* plants (Figure 6). *phyB-4* seedlings responded to EOD-FR treatments almost as well as wild-type plants did, although they were longer under all conditions (Figure 6). This result indicates that although the phyB-4 protein is impaired, its Pfr form is relatively stable in the dark in vivo. In contrast, *phyB-101* seedlings behaved as null mutants under these conditions and did not respond to EOD-FR treatments (Figure 6).

DISCUSSION

To date, virtually all of our knowledge of the biochemical and photochemical properties of phytochromes has been based on studies of phyAs purified from a few suitable etiolated plants (e.g., oats, rye, and pea). The ability to attach chromophores in vitro (Elich and Lagarias, 1989; Lagarias and Lagarias, 1989) along with the advent of recombinant phytochrome expression systems (Wahleithner et al., 1991) have opened up new avenues of research. For example, one can now study the less abundant phytochrome family members as well as phytochromes from a biochemically challenged organism like Arabidopsis. In the latter case, we can exploit the superior genetics of Arabidopsis by reconstructing missense mutations isolated in screens for impaired phytochrome activity. The detailed study of such mutant proteins provides an unexplored approach for gaining insight into phytochrome structure–function relationships.

Analysis of Arabidopsis mutants has demonstrated that phyB plays a particularly important role throughout the plant's life cycle (Reed et al., 1993; Smith, 1995). To date, screens for long hypocotyl mutants have resulted in the isolation of

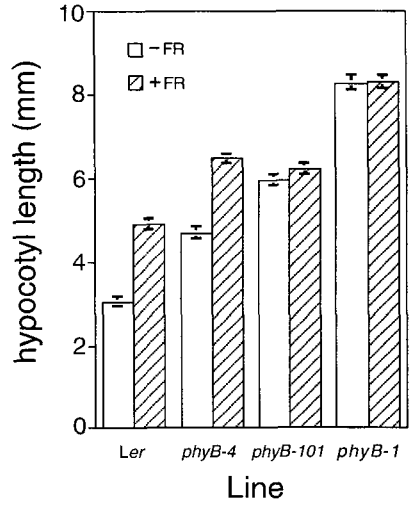

Figure 6. EOD-FR Effect on Hypocotyl Length of Wild-Type and *phyB* Plants.

Hypocotyl lengths of seedlings grown in a 10-hr-light/14-hr-dark cycle for 4 days without (open bars) or with (shaded bars) 15-min EOD-FR treatments were measured. Data are combined from two independent experiments, and each value represents the mean from measurements of 40 to 47 plants. Standard errors are indicated by error bars.

just three *phyB* missense alleles. Only two of these are presently available—*phyB-4* (Reed et al., 1993) and *phyB-101* (Bradley et al., 1996). Although both of these mutations result in a similar phenotype that is intermediate in severity relative to that of the wild type and null alleles, the respective mutations occur in distinct regions of the photoreceptor. Immunoblot analysis demonstrated that the *phyB-4* and *phyB-101* mutant phenotypes are not due to changes in phytochrome B protein levels. Therefore, a comparative analysis of the wild-type and mutant polypeptides was undertaken with the goal of elucidating the molecular basis for the mutant phenotypes.

Significant purification of the yeast-expressed Strep-tagged phyBs was attained by a single affinity chromatography step on streptavidin–Sepharose. Specific absorbance ratios ($A^{Pr}_{\lambda max}/A_{280}$, a measure of phytochrome purity) up to 0.38 were achieved, compared with the 0.79 value reported for recombinant Strep-tagged oat phyA (Murphy and Lagarias, 1997). Although we do not have an absolute phyB standard for comparison, we predict a slightly lower ratio than that of oat phyA due to the presence of an extra tryptophan residue; however, it is clear from SDS-PAGE analysis that minor levels of impurities also contribute to the lower ratios observed here. Nonetheless, the level of purity was sufficient for an informative analysis of the basic properties of this photoreceptor.

Both the native and the mutant phyBs were capable of attaching similar levels of the chromophore precursor analog PCB. Upon chromophore attachment, all three phytochromes displayed photoreversible spectrophotometric properties. The Pr–Pfr difference spectra maximum and minimum were ~650 and 712 nm in all cases, suggesting similar chromophore conformations and phototransformation reactions. These values are similar to those of 658 and 712 nm reported for tobacco phyB–PCB (Kunkel et al., 1993) as well as the 658- and 714-nm values reported for potato phyB–PCB (Ruddat et al., 1997). In contrast, the peaks observed in this study are considerably blue-shifted compared with the values of 664 and 729 nm reported for phyB in a crude extract from an Arabidopsis phyB overexpressing line (Wagner et al., 1991). A similar blue shift is seen when comparing PCB adducts of recombinant phyA to plant-derived phyA (Li and Lagarias, 1992) and is attributable to the fact that PCB contains one less double bond in its π-conjugated system than does the endogenous phyA chromophore phytochromobilin. Strictly speaking, the identity of the phyB chromophore remains unknown; however, these results are consistent with it being phytochromobilin.

Interestingly, both mutant phyBs displayed similar alterations in their spectrophotometric properties compared with wild-type phyB. This was somewhat unexpected because the mutations are in very different regions of the photoreceptor; however, unrelated defects can manifest themselves as similar changes in the measurements in question. The most obvious difference in both cases was reflected by a lower spectral change ratio. For both mutants, decreases in the Pfr extinction coefficients as well as real decreases in the photoequilibrium levels of Pfr appear to contribute to this effect. In the case of phyB-4, we currently do not understand the molecular defects that underlie these aberrant properties. We believe, however, that the detection of altered photochemical properties attributable to a single amino acid change is an important finding and should be informative in further structural studies of phytochrome phototransformation mechanisms. Furthermore, it seems likely that these altered photochemical properties are directly or indirectly related to the mutant plant phenotype. We hope, therefore, that future analysis of this mutant protein will further our understanding of phytochrome function.

Our studies with phyB-101 have been more informative and have led to a more complete understanding of the molecular defects conferred by this mutation. We have demonstrated here that recombinant phyB-101 Pfr is thermally unstable and rapidly reverts back to Pr in a nonphotochemical reaction. Recent resonance raman studies indicate that the Pfr chromophore is in a distorted, high-energy C_{15}-E, anti-configuration (Andel et al., 1996). This high-energy state is presumably stabilized through chromophore–protein interactions. Perturbation of these interactions would be expected to destabilize the Pfr chromophore, resulting in increased dark reversion. Therefore, we conclude that Glu-812 is coupled directly or indirectly to the Pfr chromophore conformation, and its mutation to a Lys residue perturbs the interactions stabilizing this conformation. This conclusion complements and extends a recent report whose findings indicate that deletion of the entire C terminus of cyanobacterial phytochrome influences chromophore conformational stability (Yeh et al., 1997).

The increased nonphotochemical reversion of Pfr would be expected to contribute directly to a lower equilibrium level of this form under any light condition. Also, the overall quantum yield for the Pfr-to-Pr phototransformation is thought to be lower than that of the primary photochemical reaction (Pfr to Meta-R) due to competing back reactions of Meta-R that may be thermal in nature (Furuya and Song, 1994). A higher energy Pfr chromophore would reduce such back reactions, leading to an increase in the overall Pfr-to-Pr quantum yield, thereby providing another mechanism by which this mutation could result in a lower photoequilibrium level of Pfr. In vivo, therefore, Pfr instability could confer a mutant phenotype for phytochrome responses dependent upon Pfr levels as well as for responses dependent upon the lifetime of the Pfr form.

Although the arguments presented above to explain the molecular basis for the *phyB-101* mutant phenotype are compelling, it was incumbent upon us to provide evidence that the results from our in vitro studies could be extended to the situation in vivo. To this end, we took advantage of the EOD-FR effect on hypocotyl elongation known to be mediated by phyB in Arabidopsis seedlings (Robson et al., 1993). By definition, such a response must be mediated by a Pfr that is relatively stable in the dark. Indeed, studies exam-

ining the effect of delaying the FR treatments have shown that even when given 6 hr after the onset of the dark period, a 50% EOD-FR response can still be observed (Casal, 1996). We have demonstrated here that *phyB-101* seedlings are null for this EOD-FR response. Because this mutant still retains phyB activity capable of inhibiting hypocotyl elongation, we conclude that the lack of this response is due to rapid dark reversion of phyB-101 Pfr in vivo similar to that observed for the recombinant protein in vitro. Together, our results suggest that decreased Pfr stability is the primary molecular mechanism conferring the *phyB-101* mutant phenotype. An interesting control for these experiments was provided by *phyB-4*, which displays a mutant phenotype similar to *phyB-101.* We have shown here that recombinant phyB-4, unlike phyB-101, did not exhibit rapid dark reversion; therefore, we predicted that *phyB-4* mutants would retain an EOD-FR response consistent with our experimental observations.

As noted previously, the *phyB-101* mutation is one of many missense mutations that cluster in a region (Quail et al., 1995) showing homology to PAS domains (Lagarias et al., 1995; Kay, 1997). This has led to speculation that this region is involved in interactions with downstream signaling machinery. Our results suggest an interesting alternative hypothesis, namely, that all of these mutations have a similar effect in destabilizing the Pfr conformation. This hypothesis can be tested in the future by reconstructing additional mutations as well as by measuring phytochrome dark reversion in extracts from overexpressing lines that have intragenic suppressor mutations in this domain (Quail et al., 1995).

In summary, we have taken a combined approach that includes genetics, biochemistry, and physiology to formulate and test a model to explain a phytochrome missense mutant phenotype. Similar studies in the future should help further our understanding of phytochrome structure and function.

METHODS

Plant Growth and Analysis

Seeds of wild-type *Arabidopsis thaliana* ecotype Landsberg *erecta* (Ler), *phyB-4* (Reed et al., 1993), *phyB-101* (Bradley et al., 1996), and *phyB-1* (Reed et al., 1993) were surface sterilized and plated on Murashige and Skoog phytagar plates (1 × Murashige and Skoog salts [Gibco Laboratories], 0.8% phytagar, and 1 × Gamborg's B5 vitamin mix). The plates were placed at 4°C in the dark for 4 days before transfer to 23°C incubators under the appropriate light conditions. For the experiment shown in Figure 1, the plants were grown for 6 days beneath a layer of nylon mesh under continuous white light at a fluence rate of 100 μmol m^{-2} sec^{-1} provided by six HO-CW fluorescent bulbs (GE Lighting, Cleveland, OH) and two 25-W incandescent bulbs. For the experiment shown in Figure 2, plates were put under continuous white light overnight and then grown in the dark for an additional 5 days. For each line, 60 seedlings were frozen in liquid nitrogen, ground to a fine powder in an Eppendorf tube using a small pestle, and extracted with 75 μL of 2 × SDS sample buffer. The samples were boiled for 2 min, microcentrifuged for 5 min, and analyzed by SDS-PAGE and immunoblotting as described below.

For the end-of-day–far-red (EOD-FR) experiments shown in Figure 6, we essentially followed published procedures (Robson et al., 1993). Replicate plates were grown beneath a layer of nylon mesh under continuous white light for 2 days at a fluence rate of 100 μmol m^{-2} sec^{-1} provided by six HO-CW fluorescent bulbs. The incubator was then set to a 10-hr-light/14-hr-dark photoperiod for an additional 4 days. During this time, at the end of every light period, one replicate plate was given a 15-min FR treatment with the spectrophotometer actinic light source described below (estimated photon fluence rate at 715 to 800 nm at 30 μmol m^{-2} sec^{-1}). For hypocotyl measurements, seedlings were sandwiched between two sheets of transparency film, and their images were scanned with a flat bed scanner. The images were analyzed with National Institutes of Health image version 1.60 software. Calibration was provided by including a ruler in the scanned images.

Phytochrome Constructs

A polymerase chain reaction (PCR) probe made with *PHYB* gene-specific primers was used to isolate a full-length *PHYB* cDNA from an etiolated Arabidopsis seedling library constructed in λ ZAPII (Kieber et al., 1993). In vivo excision according to the manufacturer's (Stratagene, La Jolla, CA) protocols yielded the plasmid p41, which contained the *PHYB* cDNA sense strand in the KpnI-to-SacI orientation in pBluescript SK− (Stratagene). The construct p41A contains a KpnI site immediately in front of the *PHYB*-initiating ATG and was made by replacing a KpnI–BstBI fragment of p41 with that from a PCR product amplified from a *PHYB* template by using the primers 5′-GTAGGTACCATGGTTTCCGGAGTC-3′ (forward, complementary to the 5′ end of *PHYB* and containing a KpnI site) and 5′-AGGCTGAATGTAACCACC-3′ (reverse internal *PHYB* primer 3′ to the unique BstBI site).

A nucleotide sequence encoding the nine–amino acid Strep-tag was then added to the 3′ end of the *PHYB* coding sequence to make the construct p41AS by replacing an EcoRI-NotI fragment of p41A with that from a PCR product amplified from a *PHYB* template using the primers 5′-GCAAATGGCTGATGGATTCG-3′ (forward internal primer 5′ to the unique EcoRI site) and 5′-ATAGTTTAGCGGCCGCTTAACCACCGAACTGCGGGTGACGCCAAGCGCTATATGGCATCATCAGCATCAT-3′ (reverse primer complementary to the codons for the last seven amino acids of PhyB and containing the coding sequence for the Strep-tag followed by a stop codon and a NotI site).

The *phyB-4* missense mutation was reconstructed by oligonucleotide-directed mutagenesis of p41A, using the oligonucleotide 5′-CTTCTCCATACTCATCTTC-3′ (antisense) according to published procedures (Kunkel et al., 1987) to yield the plasmid p41A-4. A Tth111I-MluI fragment from p41A-4, containing the mutation, was then used to replace a fragment similar to p41AS, yielding the construct p41AS-4. The *phyB-101* missense mutation was reconstructed with a QuickChange site-directed mutagenesis kit (Stratagene), according to the manufacturer's protocols, using the oligonucleotides 5′-GAACACGTGCTGCCTGAAATGGAACATGGCGATG-3′ (sense) and 5′-CATCGCCATGTTCCATTTCAGGCAGCACGTGTTC-3′ (antisense). An NsiI-SphI fragment from the resulting clone, containing the mutation, was then used to replace a like fragment of p41AS to give the construct p41AS-101. Yeast expression constructs encoding PhyB–Strep-tag (pB), PhyB-4–Strep-tag (pB4), and PhyB-101–Strep-tag

(pB101) were made by isolating KpnI-NotI fragments from p41AS, p41AS-4, and p41AS-101, respectively, and cloning them into the galactose-inducible yeast expression vector pYES2 (Invitrogen Corp., San Diego, CA). In the cloning procedures descibed above, all PCR-derived fragments that ended up in final constructs were verified by sequencing.

Expression in *Saccharomyces cerevisiae*

Plasmids pB, pB4, and pB101 were introduced into the yeast strain Invsc2 (Invitrogen) by lithium acetate transformation, according to standard protocols. For expression, several colonies were used to inoculate 5 mL of SMR (CSM-Ura, from Bio-101, containing 0.67% [w/v] yeast nitrogen base minus amino acids and 2% [w/v] raffinose). After overnight growth at 30°C with shaking, the culture was diluted into 50 mL of SMR and grown an additional day, after which the culture was diluted into 1 liter of SMG (identical to SMR except with 2% [w/v] galactose instead of raffinose). After overnight growth in SMG at 30°C with shaking, yeast cells were harvested by centrifugation at 500*g* for 5 min, washed once with ice-cold water, and stored at −80°C until use.

Phytochrome Extraction, Assembly with Chromophore, and Purification

These procedures were based on published protocols (Murphy and Lagarias, 1997). Buffers and extracts were maintained at 4°C throughout the extraction and purification procedures. Typically, extractions were performed on yeast cells from 6 liters of culture (~40 to 50 g of cells). Thawed yeast cells were resuspended in EB (50 mM Tris-HCl, pH 7.9, 100 mM NaCl, 1 mM EDTA, 1 mM EGTA, 1% [v/v] DMSO, 1 mM DTT, 1 mM benzamidine, 1.5 μg/mL leupeptin, and 2 mM phenylmethylsulfonyl fluoride) at a ratio of 0.5 mL to 1 g of cells. The suspension was added to an 80-mL bead beater chamber (Biospec Products, Inc., Bartlesville, OK) filled with 0.5-mm glass beads to a level just covering the rotor; if needed, additional beads were added to fill the remaining volume. Cells were broken with five 40-sec pulses with cooling in a dry ice–ethanol bath between the pulses. Breakage was assessed by phase contrast microscopy and typically was 70 to 95%. The slurry was filtered through two layers of Miracloth (Calbiochem, La Jolla, CA), and the beads were washed with 4 × 5 mL of EB, after which the filtrate was centrifuged for 15 min at 38,000*g*. The supernatant was removed, and 10% polyethylenimine, pH 8.0 (40 μL/mL), was added slowly with stirring. After a 10- to 15-min incubation, the mixture was centrifuged at 38,000*g* for 20 min. The supernatant was removed, and ammonium sulfate was added slowly at a ratio of 0.23 g/mL. After gentle stirring for 30 to 40 min, the ammonium sulfate precipitate (ASP) was collected by centrifugation at 12,000*g* for 20 min. The ASP pellet was resuspended in 2 to 4 mL of EB and clarified by centrifugation at 16,000*g* for 15 min. The ASP fraction was either used directly for experiments or purification or frozen in dry ice–ethanol and stored at −80°C for future use (storage up to 3 months had no deleterious effect on phytochrome activity).

Assembly with chromophores was accomplished by incubating the ASP fraction with phycocyanobilin (PCB) for 1 hr at 4°C. PCB was prepared according to published procedures (Terry et al., 1993) and added from 1 mM stock solution in DMSO to a final concentration (typically 2 to 10 μM) estimated to be in at least fivefold molar excess of phytochrome apoprotein. For purification, 100 μg/mL of avidin was added with the PCB to block biotin sites on yeast biotinylated proteins (Murphy and Lagarias, 1997). Strep-tagged phytochrome was purified using streptavidin–agarose purchased from Biometra (Tampa, FL) or prepared according to published procedures (Schmidt and Skerra, 1994). Up to 250 μg of phyB was loaded on a 1-mL bed volume column of streptavidin–agarose by gravity flow. The sample was reapplied twice, after which the column was washed with 2 × 5 mL PB (50 mM Tris-HCl, pH 7.9, 100 mM NaCl, 1 mM EDTA, and 1 mM EGTA) by gentle spinning at speed 1 in a tabletop clinical centrifuge. Bound phytochrome was eluted by gravity flow with 4 × 1-mL application of 5 mM diaminobiotin in PB. The first 1 mL of the elution fraction was discarded, and the remaining 3 mL was combined and concentrated to 0.5 to 0.7 mL by using a 50K-NMWL Ultrafree-15 centrifugal filter device (Millipore, Bedford, MA). Because the addition of cryoprotectants such as 25% ethylene glycol inhibited phyB phototransformation, samples were stored at 4°C for up to 3 days before use with no apparent loss of phytochrome photoreversibility.

Spectrophotometric Assays

Absorbance spectra were obtained with a spectrophotometer (model HP 8453 UV/visible; Hewlett-Packard Co., Palo Alto, CA). A jacketed cuvette holder was maintained at 4°C with a circulating glycol–water bath. Actinic irradiation was provided by a 100-W quartz tungsten halogen fiber optic light source (model 77500; Oriel Corp., Stratford, CT) delivered to the sample cuvette via a VIS-NIR liquid light guide (model 77636; Oriel) equipped with a collimating beam probe (model 77653; Oriel). Red irradiation was achieved by passing the light beam through a 650-nm interference filter with an 11-nm bandpass (model 53950; Oriel); FR irradiation was obtained by passage through a 715-nm-long pass filter (model 51345; Oriel) and a heat filter (model 51944; Oriel). The fluence rate for red light irradiation at the top of the sample cuvette was ~50 μmol m^{-2} sec^{-1}. For standard assays, red and FR irradiation times were 3 and 2 min, respectively. For the data presented in this study, however, irradiation times were typically 6 to 8 min and 4 min, respectively, to ensure saturation. Assuming a similar extinction coefficient as oat phyA at λ^{Pr}_{max} (132,000 M^{-1} cm^{-1}) and an M_r of 129 kD, phyB concentrations in μg/mL were approximated as $1000 \times A^{Pr}_{\lambda max}$. For dark reversion experiments, end point assays were done because the measuring beam of the spectrophotometer was found to have an actinic effect on phytochrome phototransformation. Thus, samples were irradiated with saturating red light, and Pfr spectra were acquired. The samples were then incubated in the dark for the appropriate time, after which two successive spectra were recorded. The second spectum was used to estimate the actinic effect of the measuring beam at the existing level of Pfr. This process was then repeated for the next time point. Photoreversible phytochrome levels remained unchanged over the course of these experiments.

SDS-PAGE and Immunoblot Analysis

SDS-PAGE was performed using 7.5% acrylamide minigels or 4 to 15% linear gradient precast Ready Gels (Bio-Rad). After electrophoresis, gels were either stained with Coomassie Brilliant Blue R 250 or transferred to nitrocellulose for 1 hr at 80 V. PhyB was detected using the monoclonal antibody mBA2 (Shinomura et al., 1996) followed by incubation with alkaline phosphatase–linked goat anti-mouse immunoglobulins and color development.

Steric Exclusion Chromatography

Experiments were performed at 4°C by using a Pharmacia fast-performance liquid chromatography column equipped with a UV detector and a Superdex 200 HR 10/30 column (Pharmacia Biotech Inc., Piscataway, NJ). The mobile phase buffer was 50 mM Tris-HCl, pH 7.9, 100 mM NaCl, 1 mM EDTA, and 1 mM EGTA. Pharmacia low molecular weight and high molecular weight markers were used for calibration. Absorbance difference assays were performed with the phytochrome peak fractions to verify that the protein was in a native state.

ACKNOWLEDGMENTS

We thank Drs. Clark Lagarias, John T. Murphy, and Kuo-Chen Yeh for sharing unpublished data and suggestions for phytochrome expression and purification. We are also grateful to Dr. Arne Skerra for the kind gift of recombinant core streptavidin. Finally, we thank Dr. Michael Neff for help with the construction of pB4 as well as the development of the hypocotyl measurement procedures and, along with Christian Fankhauser, for the critical reading of the manuscript. This research was supported by a grant from the National Institutes of Health (No. R01 GM52413) to J.C., who is an Associate Investigator of the Howard Hughes Medical Institute.

Received August 26, 1997; accepted October 21, 1997.

REFERENCES

Andel III, F., Lagarias, J.C., and Mathies, R.A. (1996). Resonance raman analysis of chromophore structure in the lumi-R photoproduct. Biochemistry **35,** 15997–16008.

Bradley, J.M., Murphy, G.P., Whitelam, G.C., and Harberd, N.P. (1996). Identification of phytochrome B amino acid residues mutated in three new *phyB* mutants of *Arabidopsis thaliana.* J. Exp. Bot. **47,** 1449–1455.

Casal, J.J. (1996). Phytochrome A enhances the promotion of hypocotyl growth caused by reductions in levels of phytochrome B in its FR-light–absorbing form in light-grown *Arabidopsis thaliana.* Plant Physiol. **112,** 965–973.

Cherry, J.R., Hondred, D., Walker, J.M., Keller, J.M., Hershey, H.P., and Vierstra, R.D. (1993). Carboxy-terminal deletion analysis of oat phytochrome A reveals the presence of separate domains required for structure and biological activity. Plant Cell **5,** 565–575.

Elich, T.D., and Chory, J. (1994). Initial events in phytochrome signaling: Still in the dark. Plant Mol. Biol. **26,** 1315–1327.

Elich, T.D., and Lagarias, J.C. (1989). Formation of a photoreversible phycocyanobilin-apophytochrome adduct *in vitro.* J. Biol. Chem. **264,** 12902–12908.

Fankhauser, C., and Chory, J. (1997). Light control of plant development. Annu. Rev. Cell Dev. Biol., in press.

Furuya, M., and Song, P.-S. (1994). Assembly and properties of holophytochrome. In Photomorphogenesis in Plants, 2nd ed, R.E. Kendrick and G.H.M. Kronenberg, eds (Dordrecht, The Netherlands: Kluwer Academic Publishers), pp. 105–140.

Hamazato, F., Shinomura, T., Hanzawa, H., Chory, J., and Furuya, M. (1997). Fluence and wavelength requirements for *Arabidopsis CAB* gene induction by different phytochromes. Plant Physiol. **115,** 1533–1540.

Jones, A.M., and Quail, P.H. (1986). Quaternary structure of 124-kilodalton phytochrome from *Avena sativa* L. Biochemistry **25,** 2987–2995.

Kay, S. (1997). PAS, present and future: Clues to the origin of circadian clocks. Science **276,** 753–754.

Kieber, J.J., Rothenberg, M., Roman, G., Feldmann, K.A., and Ecker, J.R. (1993). *CTR1,* a negative regulator of the ethylene response pathway in Arabidopsis, encodes a member of the Raf family of protein kinases. Cell **72,** 427–441.

Kunkel, T.A., Roberts, J.D., and Zakou, R.A. (1987). Rapid and efficient site-specific mutagenesis without phenotypic selection. Methods Enzymol. **154,** 367–385.

Kunkel, T., Tomizawa, K.-I., Kern, R., Furuya, M., Chua, N.-H., and Schafer, E. (1993). In vitro formation of a photoreversible adduct of phycocyanobilin and tobacco apophytochrome B. Eur. J. Biochem. **215,** 587–594.

Kunkel, T., Speth, V., Buche, C., and Schafer, E. (1995). In vivo characterization of phytochrome–phycocyanobilin adducts in yeast. J. Biol. Chem. **270,** 20193–20200.

Lagarias, D.M., Wu, S.-H., and Lagarias, J.C. (1995). Atypical phytochrome gene structure in the green alga *Mesotaenium caldariorum.* Plant Mol. Biol. **29,** 1127–1142.

Lagarias, J.C., and Lagarias, D.M. (1989). Self-assembly of synthetic phytochrome holoprotein *in vitro.* Proc. Natl. Acad. Sci. USA **86,** 5778–5780.

Lagarias, J.C., and Mercurio, F.M. (1985). Structure function studies on phytochrome. Identification of light-induced conformational changes in 124-kDa *Avena* phytochrome *in vitro.* J. Biol. Chem. **260,** 2415–2423.

Li, L., and Lagarias, J.C. (1992). Phytochrome assembly. Defining chromophore structural requirements for covalent attachment and photoreversibility. J. Biol. Chem. **267,** 19204–19210.

Murphy, J.T., and Lagarias, J.C. (1997). Purification and characterization of recombinant affinity-peptide-tagged oat phytochrome A. Photochem. Photobiol. **65,** 750–758.

Nagatani, A., Reed, J.W., and Chory, J. (1993). Isolation and initial characterization of *Arabidopsis* mutants that are deficient in phytochrome A. Plant Physiol. **102,** 269–277.

Parks, B.M., and Quail, P.H. (1993). *hy8,* a new class of Arabidopsis long hypocotyl mutants deficient in functional phytochrome A. Plant Cell **5,** 39–48.

Quail, P.H., Boylan, M.T., Parks, B.M., Short, T.W., Xu, Y., and Wagner, D. (1995). Phytochromes: Photosensory perception and signal transduction. Science **268,** 675–680.

Reed, J.W., Nagpal, P., Poole, D.S., Furuya, M., and Chory, J. (1993). Mutations in the gene for the red/far-red light receptor phytochrome B alter cell elongation and physiological responses throughout Arabidopsis development. Plant Cell **5,** 147–157.

Robson, P.R.H., Whitelam, G.C., and Smith, H. (1993). Selected components of the shade-avoidance syndrome are displayed in a

normal manner in mutants of *Arabidopsis thaliana* and *Brassica napa* deficient in phytochrome B. Plant Physiol. **102,** 1179–1184.

Ruddat, A., Schmidt, P., Gatz, C., Braslavsky, S.E., Gartner, W., and Schaffner, K. (1997). Recombinant type A and B phytochromes from potato: Transient absorption spectroscopy. Biochemistry **36,** 103–111.

Schmidt, T.G.M., and Skerra, A. (1994). One step affinity purification of bacterially produced proteins by means of the "Strep tag" and immobilized recombinant core streptavidin. J. Chromatogr. **676,** 337–345.

Schneider-Poetsch, H.A.W. (1992). Signal transduction by phytochrome: Phytochromes have a module related to the transmitter modules of bacterial sensor proteins. Photochem. Photobiol. **56,** 839–846.

Shinomura, T., Nagatani, A., Hanzawa, H., Kubota, M., Watanabe, M., and Furuya, M. (1996). Action spectra for phytochrome A- and B-specific photoinduction of seed germination in *Arabidopsis thaliana*. Proc. Natl. Acad. Sci. USA **93,** 8129–8133.

Smith, H. (1995). Physiological and ecological function within the phytochrome family. Annu. Rev. Plant Physiol. Plant Mol. Biol. **46,** 289–315.

Terry, M.J., Maines, M.D., and Lagarias, J.C. (1993). Inactivation of phytochrome- and phycobiliprotein-chromophore precursors by rat liver biliverdin reductase. J. Biol. Chem. **268,** 26099–26106.

Wagner, D., and Quail, P.H. (1995). Mutational analysis of phytochrome B identifies a small COOH-terminal-domain region critical for regulatory activity. Proc. Natl. Acad. Sci. USA **92,** 8596–8600.

Wagner, D., Tepperman, J.M., and Quail, P.H. (1991). Overexpression of phytochrome B induces a short hypocotyl phenotype in transgenic Arabidopsis. Plant Cell **3,** 1275–1288.

Wahleithner, J.A., Li, L., and Lagarias, J.C. (1991). Expression and assembly of spectrally active recombinant holophytochrome. Proc. Natl. Acad. Sci. USA **88,** 10387–10391.

Whitelam, G.C., Johnson, E., Peng, J., Carol, P., Anderson, M.L., Cowl, J.S., and Harberd, N.P. (1993). Phytochrome A null mutants of Arabidopsis display a wild-type phenotype in white light. Plant Cell **5,** 757–768.

Yeh, K.-C., Wu, S.-H., Murphy, J.T., and Lagarias, J.C. (1997). A cyanobacterial phytochrome two-component light sensory system. Science **277,** 1505–1508.